IDENTIFICATION OF LINEAR DYNAMIC MODELS FOR TYPE 1 DIABETES: A SIMULATION STUDY

Daniel A. Finan[†] **Howard Zisser**[‡] **Lois Jovanovic**[‡]
Wendy C. Bevier[‡] **Dale E. Seborg**[†]

[†] *Department of Chemical Engineering*
University of California, Santa Barbara
[‡] *Sansum Diabetes Research Institute*
Santa Barbara, CA

Abstract: Models of type 1 diabetes with accurate prediction capabilities can help to achieve improved glycemic control in diabetic patients when used in a monitoring or model predictive control framework. In this research, empirical models are identified from a simulated physiological model. ARX and Box–Jenkins models of various orders are investigated and evaluated for their description of calibration and validation data that are characteristic of normal operation. In addition, model accuracy is determined for abnormal situations, or "faults." The faults include changes in model parameters (insulin sensitivities), an insulin pump occlusion, underestimates in the carbohydrate content of meals, and mismatches between the actual and patient–reported timing of meals. The models describe normal operating conditions accurately, and can also detect significant faults. *Copyright ©2006 IFAC*

Keywords: Autoregressive models, biomedical systems, computer simulation, dynamic models, identification, stochastic modelling

1. INTRODUCTION

Diabetes mellitus is a disease characterized by insufficient production of insulin by the pancreatic β-cells, leading to prolonged elevated concentrations of blood glucose (Ashcroft and Ashcroft, 1992). Type 1 diabetics in particular rely on exogenous insulin for survival. This exogenous insulin typically enters the body in the subcutaneous tissue. A slow, constant or *basal* infusion helps the body metabolize glucose in times of fasting. Rapid or *bolus* injections complement the basal and are administered coincidentally with a meal to help the body metabolize large loads of carbohydrates (CHO).

Over the past few decades, many dynamic models have been formulated to describe glucose–insulin interactions in type 1 diabetes. The development of such models is relevant to a model predictive control (MPC) approach to diabetes, in which past outputs (*i.e.*, glucose measurements), past inputs (*i.e.*, insulin infusion rates), and model predictions are used to determine the appropriate insulin infusion rate at the current sampling instant (Bequette, 2005).

Physiological diabetes models include the widely used "minimal model" of Bergman *et al.* (1981), which was developed to estimate insulin sensitivity from an intravenous glucose tolerance test. The model describes glucose–insulin dynamics with only three differential equations and

few parameters. This simplicity, however, begets many limitations. For instance, the original model excluded exogenous insulin infusion as an input. Although it has been easily altered to include this input (Parker and Doyle III, 2001), the modified minimal model still does not include the dynamics of subcutaneous insulin infusion. A more recent model by Cobelli *et al.* (1998) is significantly more detailed than the model of Bergman *et al.* (1981), but its details are thus far unpublished. A physiologically rigorous 19–state model was developed by Sorensen (1985) to describe glucose–insulin pharmacokinetics/pharmacodynamics, and includes compartments representative of various bodily organs. Shortcomings of this model include its inability to capture the realistic hyperglycemic extremes characteristic of type 1 diabetes (Lynch and Bequette, 2002). A model developed by Hovorka (Hovorka *et al.*, 2002; Hovorka *et al.*, 2004) presents an attractive tradeoff between simplicity and accuracy. This model is the focus of the current research.

In addition to physiological diabetes models, empirical diabetes models have also been reported, although to a much lesser extent. Autoregressive models have been used to predict the next glucose value (ten minutes ahead) from previous glucose measurements (Desai *et al.*, 2002). The novelty of the current paper is that different types of models are considered (namely ARX and Box–Jenkins) and only "infinite–step ahead" model predictions are evaluated. That is, the empirical models predict future outputs based only upon the process inputs and the previous empirical model outputs; thus, the actual outputs (from the Hovorka model) are not used to update the empirical model predictions.

2. PHYSIOLOGICAL MODEL

The diabetes model considered in this research is the model reported by Hovorka *et al.* (2004) and extended by Wilinska *et al.* (2005). The model inputs are the rate of subcutaneously infused insulin lispro (fast acting insulin), and meal amount and time. The output is the plasma glucose concentration. The model is comprised of three subsystems representing plasma glucose, subcutaneous and plasma insulin, and insulin action. The glucose subsystem is divided into two compartments, a plasma compartment and a "non–accessible" compartment; subcutaneous insulin absorption is also partitioned into two compartments. The insulin action subsystem takes into account the physiological effects of insulin on glucose transport, removal, and endogenous production. These insulin "actions" manifest themselves in the form of

time–varying rate constants corresponding to each of these metabolic processes. Model "constants" were taken to be those quantities which were difficult to identify, while model "parameters" were *a priori* identifiable. Nonlinearity arises in the model not only from the insulin actions but also from physiological saturation effects. For example, renal glucose excretion is zero below a certain threshold (160 mg/dL) and insulin–independent peripheral glucose uptake is constant above, and proportional to glucose concentration below, another threshold (80 mg/dL). The model also includes gut absorption dynamics which describe the appearance of glucose in the blood resulting from a meal. The model's subcutaneous insulin absorption subsystem includes parallel fast and slow channels as well as a degree of insulin degradation at the injection site.

Figure 1 shows the steady–state map of plasma glucose concentration (G) and insulin infusion rate (u) predicted by the Hovorka model for three different patient weights. Three operating regions are evident in the model. In Region 1 ($G \geq 160$ mg/dL), renal glucose excretion is present and proportional to G; in Regions 2 and 3 ($G \geq 80$ mg/dL), non–insulin–dependent glucose uptake is constant; and in Region 3 ($G < 80$ mg/dL) non–insulin–dependent glucose uptake is proportional to G. Figure 1 indicates that the model produces negative glucose concentrations for high insulin infusion rates. Although negative glucose concentrations are unrealistic, the model is intended to be operated at physiological glucose levels, *e.g.*, 40 mg/dL $< G <$ 400 mg/dL.
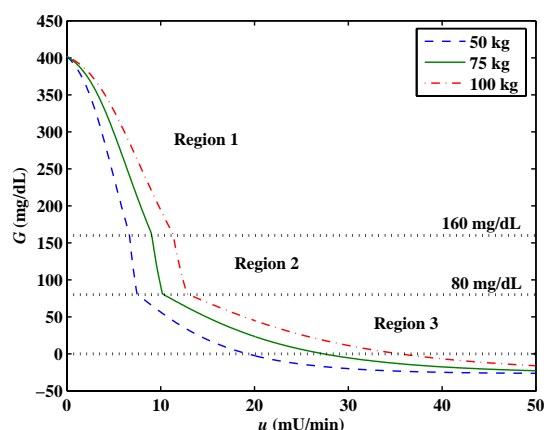

Fig. 1. Steady–state G–u map for three patient weights. Regions 1-3 represent different operating regions for the model.

Transient responses to open–loop changes in the insulin infusion rate u were simulated in order to characterize the insulin–to–glucose dynamics of the Hovorka model. Figure 2 shows the responses of G to step changes in u (*i.e.*, basal changes) and an impulse in u (*i.e.*, a bolus). The step

and impulse magnitudes were chosen so that the process operated entirely within Region 2 (see Figure 1), the most physiologically significant region. Figure 2 indicates that ∼75 h are required for G to reach steady state in response to the step decrease in u, but only about half this time is required to reach steady state after the step increase in u.
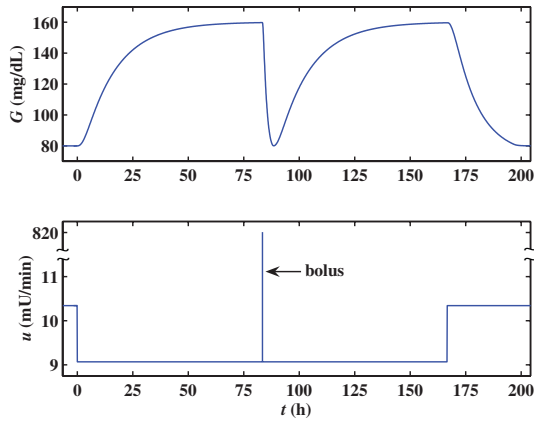

Fig. 2. Transient glucose responses for a 75 kg patient to open–loop step (basal) and impulse (bolus) inputs in u. Note broken scale in the input plot.

Transient responses to a meal disturbance were simulated in order to characterize the *postprandial* (*i.e.*, post–meal) glucose concentration dynamics. Figure 3 shows two responses to a 40 g CHO meal: an open–loop response for which no counteracting bolus is delivered, and the response when an appropriate bolus is delivered coincident with the meal. The rate of appearance of glucose in the blood from the meal U_G is the prediction of the model's gut absorption subsystem. Since using impulse inputs for both boluses and meals could cause identifiability problems, the input for a meal is considered to be U_G. The insulin–to–carbohydrate ratio for the bolus was determined by trial and error such that the bolus significantly reduced the postprandial peak and returned G to its steady–state value quickly, without significant undershoot.

2.1 Normal Operation

In order to simulate days of normal operation, certain assumptions had to be made regarding what is "normal." All runs simulated a 24 h period, starting at 8 AM and ending the following day at 8 AM. The sampling period was 5 min, a realistic interval for the current generation of continuous glucose sensors. Gaussian noise was added to the glucose measurement, with a standard deviation of $\sigma = 3.3$ mg/dL. Breakfast, lunch, and dinner were administered at 8 AM, 12 PM, and 6 PM,
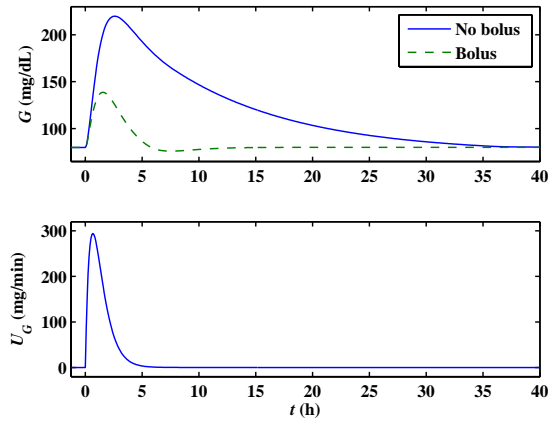

Fig. 3. Transient glucose responses for a 75 kg patient to meal input U_G, with and without a coincident bolus.

respectively. All normal runs used the nominal insulin sensitivities reported by Hovorka *et al.* (2002) and Hovorka *et al.* (2004). The patient weight was 75 kg. Three "normal" datasets were simulated corresponding to an *average meal day* (N_A), a *light meal day* (N_L), and a *heavy meal day* (N_H). In the light meal day, the simulated patient consumes 50% less CHO in each meal compared to the average meal day; in the heavy meal day, the patient consumes 50% more CHO in each meal compared to the average meal day. The insulin–to–carbohydrate ratio was constant for each meal, and was determined as described above.

2.2 Faults

The four realistic "faults" in Table 1 were simulated, representing changes in model parameters (insulin sensitivities), an insulin pump occlusion, patient underestimates of the amount of CHO consumed in meals, and mismatches between the actual timing of meals and that which the simulated patient reports to a hypothetical monitoring system. The same Gaussian noise level, meal times, and patient weight were used in the fault datasets as in the normal datasets.

Table 1. Fault descriptions.

Fault	Description
$F1$	50% reduction in insulin sensitivities
$F2$	100% occlusion of insulin pump for one hour (not during a meal)
$F3$	50% underestimate in CHO content of lunch and dinner
$F4$	15 min mismatch between actual and patient–reported lunch and dinner times

For the $F1$ fault simulation, an appropriate basal rate and insulin–to–carbohydrate ratio were recalculated to compensate for the decreased insulin

sensitivities. For $F2$, the basal insulin infusion rate was completely stopped for one hour, from 12 AM to 1 AM. The u input data used to generate the empirical model prediction, however, do not include this hour–long cessation in the basal. Here the assumption is that an online monitoring system would not be aware of the occlusion, and thus would be challenged to infer it from the available input–output data. Faults $F1$ and $F2$ were generated using the meal magnitudes for a normal, average meal day. For $F3$, lunch and dinner were two times larger than average and were taken with coincident boluses appropriate for the average–sized meals (*i.e.*, the patient underbolused for lunch and dinner). Since the patient underestimated these actual meal amounts by 50%, both the u and U_G input data used to generate the empirical model prediction for $F3$ are the same as for a normal average meal day. For fault $F4$, the lunch and dinner boluses were taken at their nominal times, but the meals were taken 15 min late (*i.e.*, after the boluses). Again, the assumption here is that an online monitoring system would not be aware of these mismatches in meal timing, and thus would be challenged to infer them. Therefore, the input data used to generate the empirical model prediction for $F4$ were the same as for a normal average meal day.

3. EMPIRICAL MODELS

The two types of linear dynamic models investigated in this research are autoregressive models with exogenous input (ARX) and Box–Jenkins (BJ) models. The MATLAB System Identification Toolbox (Ljung, 2005) was used to identify the models. The ARX model is a difference equation in which the current output depends on previous outputs and inputs,

$$
\begin{aligned}
A(q^{-1})G(t) = &\ B_1(q^{-1})u(t) \\
&+ B_2(q^{-1})U_G(t) + \varepsilon(t)
\end{aligned} \tag{1}
$$

where q^{-1} is the backward shift operator (*i.e.*, $q^{-1}G(t) = G(t-1)$). A is a scalar polynomial in ascending powers of q^{-1}, starting with $q^0 = 1$ and B_1 and B_2 are scalar polynomials in ascending powers of q^{-1}, starting with q^{-1}. The ε term represents the Gaussian process noise. Low–order and high–order ARX models were identified from the Hovorka model simulation data. The "low–order" models were second order in the autoregressive and exogenous inputs; the "high–order" models were chosen according to the Akaike information criterion (AIC), which chooses model orders based on a compromise between model simplicity and model accuracy.

The BJ model is a transfer function model that models both deterministic inputs (*i.e.*, u and U_G) and stochastic inputs (*i.e.*, the noise ε) according to

$$
\begin{aligned}
G(t) = &\ \frac{B_1(q^{-1})}{F_1(q^{-1})}u(t) \\
&+ \frac{B_2(q^{-1})}{F_2(q^{-1})}U_G(t) + \frac{C(q^{-1})}{D(q^{-1})}\varepsilon(t)
\end{aligned} \tag{2}
$$

where B_1, B_2, C, D, F_1, and F_2 are scalar polynomials in ascending powers of q^{-1}, starting with q^{-1}. Again, low–order and high–order BJ models were identified from Hovorka model simulation data. The "low–order" BJ models were first order in all inputs while the "high–order" models were fourth order.

For the identification studies, deviation variables were used. Because the physiological model does not account for the diurnal variations in insulin sensitivities, the basal insulin infusion rate was constant for the entire day. Since this steady–state infusion rate was subtracted in forming deviation variables, the input u consisted only of impulses (*i.e.*, boluses). The steady–state value of $G = 80$ mg/dL was subtracted from the output to give the deviation variable ΔG.

4. SIMULATION RESULTS

Model accuracy for both calibration and validation data was quantified by the standard coefficient of determination,

$$
R^2 = \left(1 - \frac{\sum_{i=1}^{N}(G_i - \hat{G}_i)^2}{\sum_{i=1}^{N}(G_i - \bar{G})^2}\right) \times 100\% \tag{3}
$$

where N is the number of samples, G is the output simulated by the Hovorka model, $\hat{G}$ is the output predicted by the identified model, and $\bar{G}$ is the average of the output simulated by the Hovorka model.

Low–order and high–order ARX and BJ models were identified from each of the three datasets representative of normal operation (*i.e.*, N_A, N_L, and N_H). Each of the twelve identified models was validated on the other two normal datasets. Figure 4 compares the predictions of the high–order models identified from N_A with all three normal datasets. The corresponding R^2 values are listed in Table 2 and range from 46-77%.

The R^2 values of the high–order ARX and BJ models for the three normal datasets are shown in Table 2. Both types of models predict their calibration data accurately ($R^2_{cal} \geq 66\%$, $\bar{R}^2_{cal} = 74.5\%$) In general, the BJ models consistently
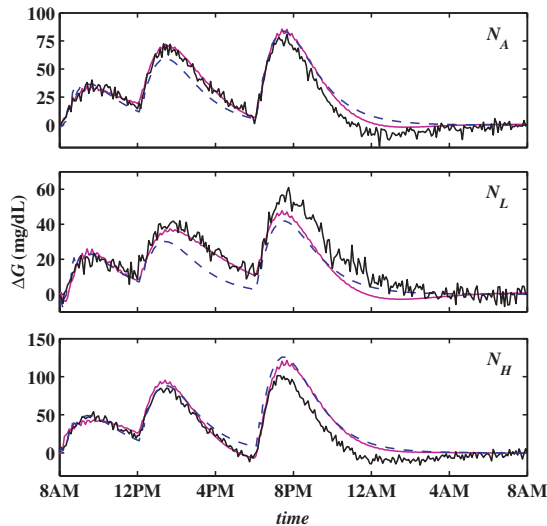
Fig. 4. Comparison of Hovorka model responses and predictions of high–order models identified from N_A. Top: calibration data; middle (N_L) and bottom (N_H): validation data. BJ: thin solid line; ARX: dashed line. Note different scales in the y–axes.

explain more variability in the data than the ARX models. The worst prediction occurs when the ARX model identified from N_L is validated on N_H. Here $R^2 = 0$, implying that the model prediction is no more accurate than the average value of the simulation data.

Table 2. R^2 values of predictions of high–order models identified from N_A for all normal datasets. Boldface values denote results for calibration data.

Day	Model	N_A	N_L	N_H
N_A	ARX	**66**	46	57
	BJ	**77**	57	63
N_L	ARX	32	**74**	0
	BJ	52	**78**	42
N_H	ARX	62	27	**74**
	BJ	71	68	**78**

The R^2 values of the low–order ARX and BJ models for the three normal datasets are shown in Table 3. The low–order model fits are comparable to those of the high–order models ($\bar{R}^2_{high} = 56.9$; $\bar{R}^2_{low} = 59.7$).

The models identified from the N_A dataset were evaluated on the fault datasets simulated by the Hovorka model. The predictions of the identified high–order models are shown in Figure 5, and the corresponding R^2 values are listed in Table 4. Very low R^2 values imply that the identified model is not accurate and that an abnormal situation (*i.e.*,

Table 3. R^2 values of predictions of low–order models identified from N_A for all normal datasets. Boldface values denote results for calibration data.

Day	Model	N_A	N_L	N_H
N_A	ARX	**66**	43	58
	BJ	**71**	70	79
N_L	ARX	38	**70**	7
	BJ	62	**78**	58
N_H	ARX	61	27	**72**
	BJ	71	66	**80**

fault) has occurred. The high–order ARX model easily detects $F3$, while the high–order BJ model detects $F1$ and $F3$. Although both identified models still explain $\sim 50\%$ of the variance in $F2$, these R^2 values are significantly lower than the corresponding calibration values (see Table 2). It should also be noted that most of the unexplained variance comes in the last ~ 6 h of the $F2$ run, *i.e.*, after the pump occlusion occurs at 12 AM. In an online monitoring situation, recent data would typically be weighted more heavily, and this fault would likely be detected soon after it occurs. Finally, $F4$ goes undetected, illustrating a degree of insensitivity of the identified models. A reasonable amount of insensitivity is advantageous because the detection of an insignificant fault situation is undesirable.
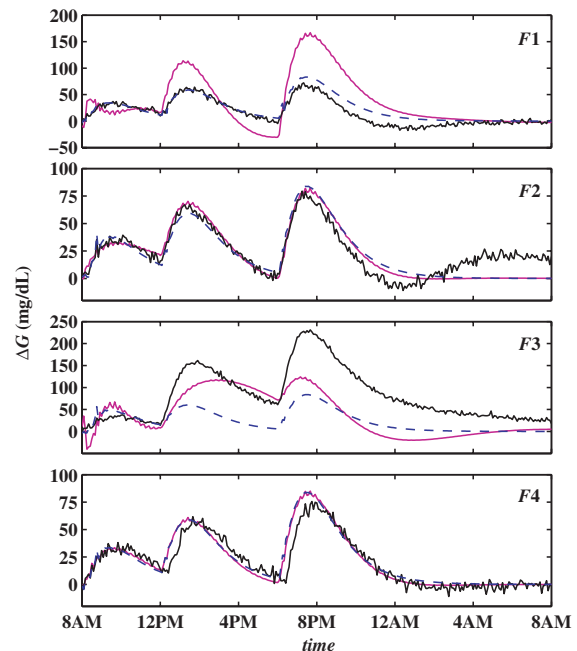

Fig. 5. Validation results for high–order models identified from N_A for $F1$ (top), $F2$ (middle top), $F3$ (middle bottom), and $F4$ (bottom). BJ: thin solid line; ARX: dashed line. Note different scales in the y–axes.

Table 4. R^2 values of predictions of all models identified from N_A, evaluated for the fault datasets.

Order	Model	$F1$	$F2$	$F3$	$F4$
High	ARX	53	48	-20	61
Order	BJ	-63	51	-2	64
Low	ARX	54	47	-21	60
Order	BJ	68	52	61	63

The R^2 values of the low–order ARX and BJ models identified from N_A evaluated on the four fault datasets are also shown in Table 4. The R^2 values are significantly higher than those of the high–order models ($\bar{R}^2_{high} = 11.2$; $\bar{R}^2_{low} = 43.5$).

5. CONCLUSIONS

Accurate linear dynamic models have been identified from a simulated physiological diabetes model. The simulations represented realistic conditions by incorporating measurement noise, reasonable meal times and magnitudes, insulin–to–carbohydrate ratios, and faults. The high–order ARX and BJ models identified from the normal data provide accurate predictions of the normal datasets. The low–order model predictions of the normal datasets are comparable to those of the high–order models.

The models identified from N_A were applied to the four fault datasets to determine whether a distinction could be made between normal operation and faults. Two of the four faults ($F1$ and $F3$) were detected readily by the high–order models. $F2$ was more difficult to detect by the high–order models, in part because the fault occurred near the end of the run. Finally, $F4$ went undetected due to the insignificance of this fault. The low–order models developed from N_A largely failed to distinguish between normal operation and faults.

ACKNOWLEDGEMENTS

REFERENCES

Ashcroft, F.M. and S.J.H. Ashcroft (1992). *Insulin: Molecular Biology to Pathology*. Oxford University Press. New York, NY.

Bequette, B.W. (2005). A critical assessment of algorithms and challenges in the development of a closed–loop artificial pancreas. *Diabetes Technol Ther* **7**(1), 28–47.

Bergman, R.N., L.S. Philips and C. Cobelli (1981). Physiological evaluation of factors controlling glucose tolerance in man. *J Clin Invest* **68**(6), 1456–1467.

Cobelli, C., G. Nucci and S. Del Prato (1998). A physiological simulation model of the glucose–insulin system in type I diabetes. *Diabetes Nutr Metab* **11**(1), 78.

Desai, S., J. Tamada, R. Kurnik and R. Potts (2002). Predicting glucose values from previous measurements. *Diabetes Technol Ther* **4**, 215.

Hovorka, R., F. Shojaee-Moradie, P.V. Carroll, L.J. Chassin, I.J. Gowrie, N.C. Jackson, R.S. Tudor, A.M. Umpleby and R.H. Jones (2002). Partitioning glucose distribution/transport, disposal, and endogenous production during IVGTT. *Am J Physiol Endocrinol Metab* **282**(5), E992–1007.

Hovorka, R., V. Canonico, L.J. Chassin, U. Haueter, M. Massi-Benedetti, M.O. Federici, T.R. Pieber, H.C. Schaller, L. Schaupp, T. Vering and M.E. Wilinska (2004). Nonlinear model predictive control of glucose concentration in subjects with type 1 diabetes. *Physiol Meas* **25**(4), 905–20.

Ljung, L. (2005). *System Identification Toolbox*. 6 ed. The MathWorks, Inc. 3 Apple Hill Drive, Natick, MA 01760-2098.

Lynch, S.M. and B.W. Bequette (2002). Model predictive control of blood glucose in type I diabetics using subcutaneous glucose measurements. In: *Proceedings of the American Control Conference*. pp. 4039–4043.

Parker, R.S. and F.J. Doyle III (2001). Control–relevant modeling in drug delivery. *Adv Drug Deliv Rev* **48**, 211–228.

Sorensen, J.T. (1985). A physiologic model of glucose metabolism in man and its use to design and assess improved insulin therapies for diabetes. PhD thesis. Massachusetts Institute of Technology.

Wilinska, M.E., L.J. Chassin, H.C. Schaller, L. Schaupp, T.R. Pieber and R. Hovorka (2005). Insulin kinetics in type–1 diabetes: Continuous and bolus delivery of rapid acting insulin. *IEEE Trans Biomed Eng* **52**(1), 3–12.